

Interference optical measurements during continuous and discontinuous crack propagation in fatigue loaded polymers

L. KÖNCZÖL, M. G. SCHINKER, W. DÖLL

Fraunhofer-Institut für Werkstoffmechanik, Wöhlerstrasse 11, D-7800 Freiburg, West Germany

Continuous and discontinuous fatigue crack propagation behaviour have been investigated in PMMA and PVC, respectively, using the optical interference method. Thus craze zone sizes at the crack tip have been measured as functions of cycle number and relative stress intensity factor during crack propagation and between crack jumps. The results obtained give new and improved information on the material behaviour in the micro-region at the crack tip and also lead to modifications of a previously proposed model on crack and craze propagation behaviour during fatigue.

1. Introduction

During crack growth in fatigue loaded polymers two types of fatigue crack propagation (FCP) behaviour have been observed [1, 2].

During the so-called continuous FCP, at every loading cycle an increase in crack length occurs, whereas during the so-called discontinuous FCP the crack front advances an increment after remaining stationary for a great number of fatigue cycles*. Which type of fatigue crack growth occurs has been found to depend on the polymer investigated, the magnitude of relative stress intensity factor, ΔK_I , and frequency [3].

Besides these macroscopic characterizations deeper insights have been obtained by microscopic [4] and microscopic interference [5, 6] investigations in measuring the development of the craze length at the crack tip after the specimens have been loaded in fatigue. In order to utilize all the benefits of the optical interference method, which also gives information on the craze and crack openings and hence on lengths of stretched fibrils, measurements have to be performed during fatigue crack propagation. This requires a more elaborate experimental arrangement to record all relevant parameters simultaneously during fatigue crack

propagation. Such an experimental set-up has been built and described previously and results have been reported for PMMA [7-9].

The aim of this paper is to present new or improved information on the material behaviour in the micro-region at the crack tip measured during continuous and discontinuous fatigue crack propagation in PMMA and PVC using the optical interference method.

2. Experimental details

The experiments were performed on commercial grades of PMMA of high molecular weight (Plexiglas 233, supplied by Röhm, Darmstadt) and of PVC (Vestolit 3869 B with molecular weights of number average molar mass $\bar{M}_n = 1.37 \times 10^4$ and weight average molar mass, $\bar{M}_w = 3.43 \times 10^4$ supplied by Chemische Werke Hüls, Marl). Miniature CT-specimens were used and loaded by tensile fatigue (2 Hz, sine wave with the lower load limit about 5% of the upper tensile load, thus giving a very low R ratio) at room temperature (23°C, 50% r.h.).

To characterize the macroscopic fatigue crack propagation behaviour of the two materials under the applied load conditions, Fig. 1 shows the

*Basically both types of FCP are discontinuous; hence the so-called "discontinuous" type would be better characterized as "retarded" crack growth.

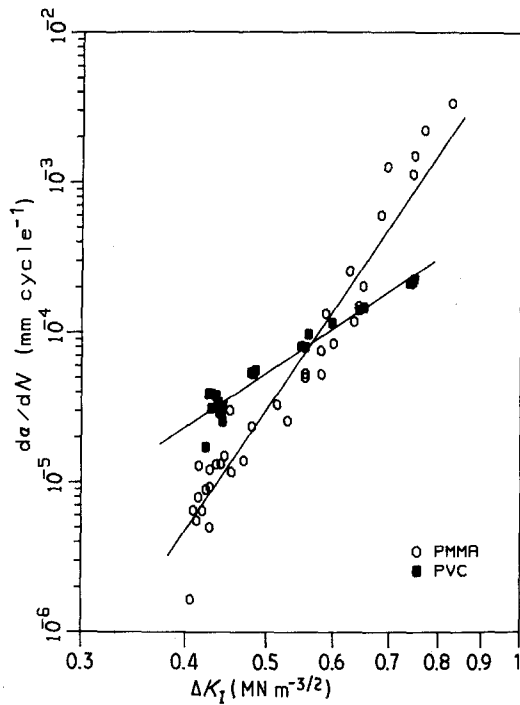


Figure 1 Fatigue crack propagation rate da/dN as a function of relative stress intensity factor ΔK_I at 2 Hz.

measured increase in crack length, da , per number of cycles, dN , against relative stress intensity factor, ΔK_I . Comparing these curves with the data of other authors [3], it can be stated that they are in the same range. However, the PMMA curve here is shifted a little bit to higher ΔK_I values and the PVC curve here has a steeper slope.

Simultaneously with the registered situation of fatigue crack propagation the interference fringe pattern was recorded (see Fig. 6). Due to the experimental arrangement the interference fringe pattern can be taken at any phase of the cyclic load. Usually it was recorded at upper and lower load. Details of the applied evaluation procedure of the fringe pattern have been described together with those of specimen preparation [10].

3. Results and discussion

The macroscopic fatigue crack growth behaviour of the two materials investigated is shown in Fig. 1. It is obvious that this kind of plot, although commonly used, does not exhibit the basic difference between continuous and discontinuous crack growth.

3.1. Continuous fatigue crack growth in PMMA

The following sheds some light on the craze zone size at the crack tip during so-called continuous FCP in PMMA. Fig. 2 shows the evaluated contours of craze zone measured at lower and upper load ($\Delta K_I = 0.68 \text{ MN m}^{-3/2}$). The increase in crack length is not indicated, and it should be mentioned that crack growth occurs mainly during a time interval before and after maximum load [11]. From Fig. 2 it can be seen that during one loading cycle the craze length is nearly constant (due to the fact that at the same rate bulk material is fibrillated and craze material fails) while the craze thickness changes by nearly 100%. The

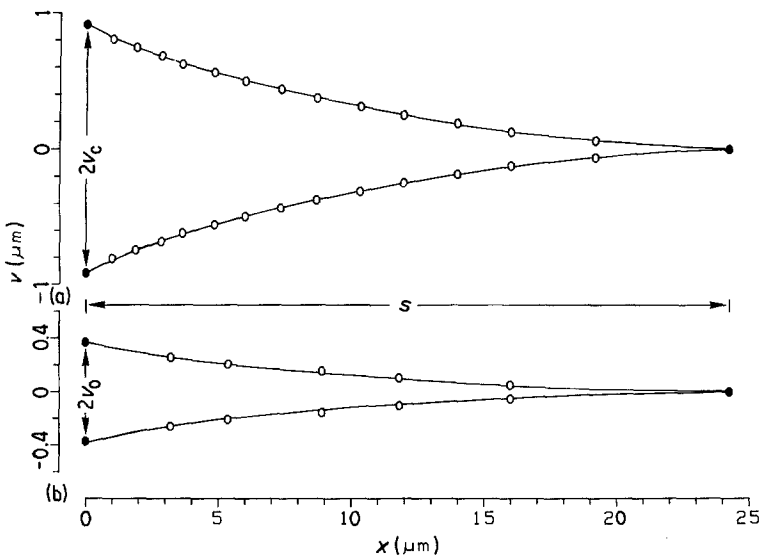


Figure 2 Craze contour at the crack tip in PMMA during fatigue loading at (a) upper and (b) lower load, as measured by interference optics.

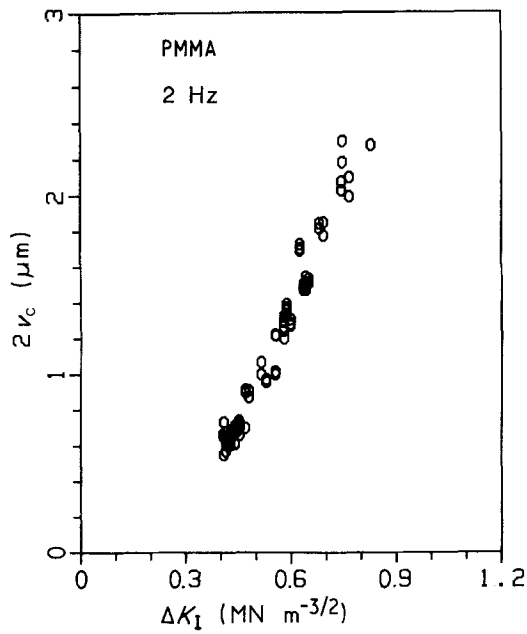


Figure 3 Maximum craze width $2v_c$ at the crack tip as a function of relative stress intensity factor ΔK_I .

dependence of maximum craze width $2v_c$ (at upper load) on relative stress intensity factor ΔK_I is shown in Fig. 3. It can be seen that during fatigue crack propagation in high molecular weight PMMA the maximum craze width, $2v_c$, and hence also the crack opening stretch is not constant but increases by a factor of nearly 5 (from $0.5 \mu\text{m}$ to about $2.4 \mu\text{m}$) in the predominantly investigated stress intensity range between 0.4 and $0.8 \text{ MN m}^{-3/2}$. Fig. 3' suggests a lower limit of $2v_c$ at ΔK_I values lower than $0.5 \text{ MN m}^{-3/2}$. It has been shown [9] that an upper limit of $2v_c$ is given obviously by the craze size of continuously moving cracks under quasi-static load, which has been determined for this PMMA to be nearly constant at $2v_c = (2.7 \pm 0.2) \mu\text{m}$ [12].

Referring to the fatigue striation spacing on the fracture surfaces of PMMA which represents the increase in crack length during one loading cycle (continuous FCP) the measured results show no simple and systematic correlation between striation spacings and craze dimensions [9]. Thus, in a wide range of low propagation rates the craze dimensions are larger than the advance in crack length during one cycle. At crack propagation rates higher than $3 \times 10^{-2} \text{ mm cycle}^{-1}$, however, the length of the existing craze zone is always smaller. In this context the following observation [11] may be very helpful for an understanding of

the fatigue crack propagation mechanism: during one loading cycle when the crack advances an increment into the already formed craze material at the craze base then almost simultaneously at the craze tip bulk material is transformed into new craze material leading to an unchanged length of the craze zone at constant ΔK_I . An increase or decrease in craze length depends on the ΔK_I level applied as may be seen from [9]. If the ΔK_I level is high enough then a situation as in continuous crack propagation under constant load may arise leading to a constant length of the craze zone although the K_I level still increases [12].

It has been shown [9] that during continuous FCP in PMMA the two characteristic craze dimensions (i.e. maximum width and length) remain practically proportional to one another. The increase in craze length occurs by fibrillation of amorphous bulk material, whilst the thickening of the craze occurs by additional fibrillation as well as by stretching of the already formed fibrils. It is interesting to note that the strain on the stretched fibrils increases with increasing ΔK_I [9].

It has to be emphasized that during continuous FCP the maximum craze widths $2v_c$ represent the critical lengths of stretched molecular fibrils spanning the crack tip in the moment of crack propagation.

3.2. Discontinuous fatigue crack growth in PVC

3.2.1. Behaviour between crack jumps

On the other hand during discontinuous FCP in which the crack tip remains stationary for several hundred loading cycles before jumping at a particular cycle, the craze sizes were in most cases observed at the crack tip being already or still stationary. Thus Fig. 4 shows a sequence of craze contours determined in PVC at times of upper load between two successive crack jumps and hence at constant ΔK_I . It can be seen from Fig. 4 that the craze increases in size with increasing number of loading cycles, N . The development of characteristic craze dimensions (length s and maximum craze width denoted here as $2v$), determined by extrapolation, are given in Fig. 5 as functions of cycle number N , for several successive crack jumps. In this experiment ($\Delta K_I = 0.48 \text{ MN m}^{-3/2}$) the crack remained stationary up to a critical cycle number N_e of 410 to 500 cycles. N_e is connected with a critical end length s_e or end width $2v_e$ respectively. From Fig. 5 it can be seen that between

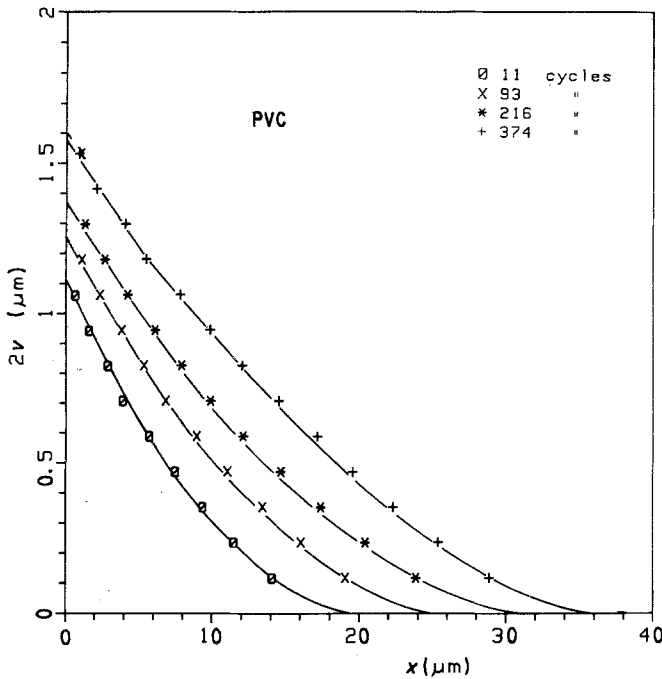


Figure 4 Measured craze contour at the crack tip in fatigue loaded PVC ($\Delta K_I = 0.48 \text{ MN m}^{-3/2}$) after different loading cycles N .

two successive crack jumps the craze grows continuously in length, demonstrated previously [3, 13], as well as in thickness. From Fig. 5 it is rather obvious that the crack does not go through the craze all the way up to the craze tip as was usually assumed [3, 13]. It stops well ahead of the craze tip [6] even at this low R ratio. This crack propagation behaviour is demonstrated more clearly by the optical interference photograph in Fig. 6 taken at the very moment of a crack jump. In the upper part of the photograph the crack is still stationary with the craze having its full length, while in the lower part the crack has already moved forward. The dynamics of the process reminds one of the opening of a zip-fastener. In order to localize the exact position of the crack tip

and hence the length of the craze zone from such a photograph it is very helpful to apply a microdensitometer. Figs. 7a and b give the densitometer traces of the interference fringe pattern from the upper and lower part of the photograph in Fig. 6. Knowing that the distances between the maxima and minima form a decreasing pattern going along the trace towards the crack tip from the craze zone as well as from the crack opening, the position of the crack tip can be identified. Thus, it can clearly be seen that the crack does not jump through the craze zone up to the craze tip. By comparing the upper and lower part of Fig. 6 it is obvious that in this case the crack separates the fibrillar craze matter up to about two thirds of the craze length without penetrating into the front

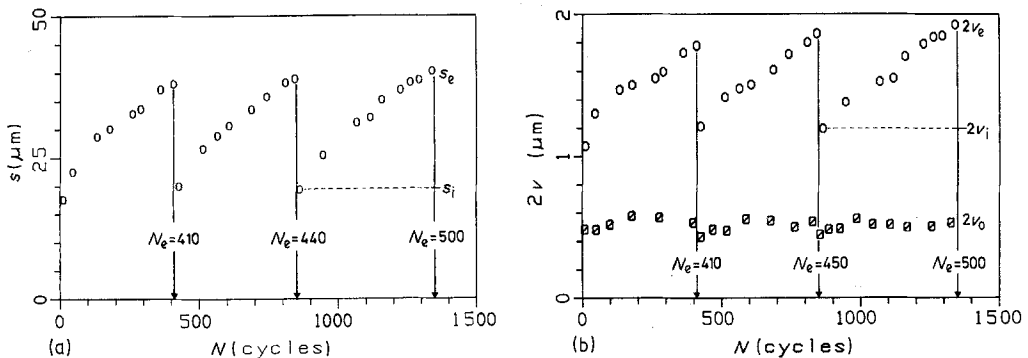


Figure 5 Craze growth as function of loading cycles N between successive crack jumps, in PVC at $\Delta K_I = 0.48 \text{ MN m}^{-3/2}$. (a) Craze length s , (b) craze width direct at the crack tip under upper ($2v_i$ to $2v_e$) and lower ($2v_0$) load.

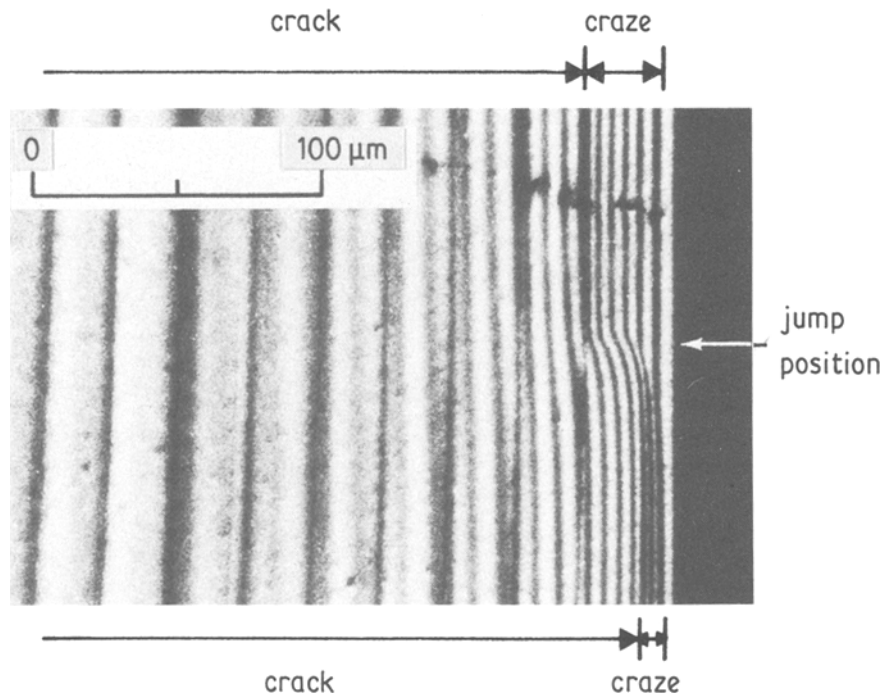


Figure 6 Interference fringe pattern taken at the very moment of a crack jump in PVC (superimposed by fatigue bands on the fracture surface).

part of the craze. Additionally it can be noticed that at the position of the new crack front the maximum craze width is larger than at the original craze position. This can also be seen directly from the order of fringes at the position of the new crack tip. An exact evaluation of the photograph shows that a small increase in length must have occurred also during the crack jump. From Fig. 5 it can more precisely be derived that just after a crack jump the craze starts to lengthen with an initial craze length s_i of nearly 50% of the old length; thickening begins with an initial value $2v_i$ of nearly 60%. These relative differences between the initial length and width of the craze have to be seen as a direct effect of the crack jump and are balanced by the following growth behaviour. After an initially steeper increase in craze length, further craze growth occurs relatively linearly up to the critical end dimensions.

As a consequence of these results the proposed model [3, 4, 13] of discontinuous crack growth in fatigue must be essentially modified [11]. Fig. 8 shows the two basic stages of craze size during FCP. The one stage is characterized by the big

craze size (s_e and $2v_e$) just before a crack jump occurs and when the position of the crack tip is still at $2v_e$. The other stage is characterized by the small craze size (s_i and $2v_i$) just after a crack jump has occurred and when the position of the crack tip is then at $2v_i$. As already discussed qualitatively above it can be concluded from Fig. 8 that the crack jumps only partly through its old big craze and that during the jump the crack induces an increase in the remaining craze part. The given craze dimensions refer to a ΔK_I value of $0.48 \text{ MN m}^{-3/2}$. The principal result holds for all situations of discontinuous FCP investigated. However, the dimensions will change with ΔK_I (see below). After the crack jump the initial craze (s_i and $2v_i$) increases continuously*) ([3, 4, 13] and Fig. 5) up to that size when the crack again advances an increment. From Figs. 6 and 8 it can be seen directly that the increase in crack length (= band width, b , on the fracture surface) is not equal to the craze length and hence this former interpretation [1, 3] must be modified (see below).

In order to obtain information on the sudden

*"Continuous" craze growth has to be seen in relation to the "discontinuous" crack growth; looking at a finer scale, e.g. at one loading cycle, then discontinuous craze growth is to be expected [11].

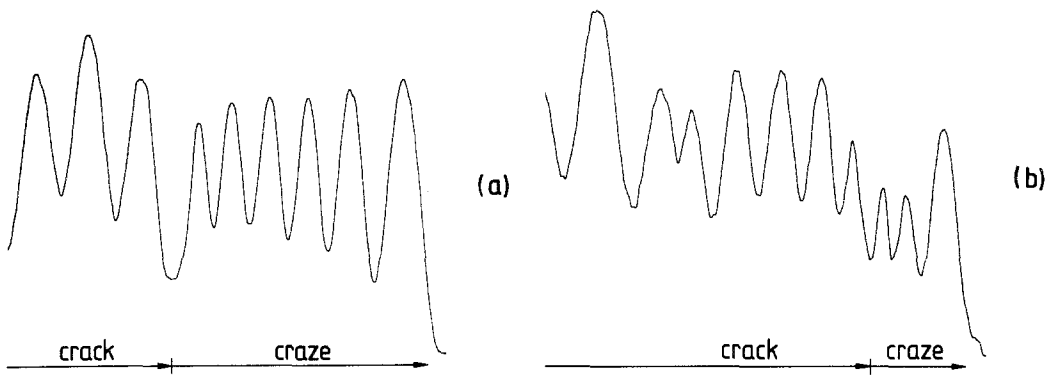


Figure 7 Microdensitometer traces of crack and craze opening shown in Fig. 6: (a) before crack jump, and (b) after crack jump.

breakdown of the craze after a long sustaining period of several hundred loading cycles it is helpful to analyse the craze growth in detail between two successive crack jumps. Obviously the craze lengthening takes place by fibrillation of amorphous bulk material. The thickening of the craze may be due to an additional fibrillation of bulk material or due to enhanced stretching of already formed fibrils, or possibly due to both processes. To investigate this question the craze width, $2v_0$ at the crack tip was determined under lower load. $2v_0$ can be regarded as a direct measure of the amount of fibrillated material. The measured data shown in Fig. 5b strongly suggest a constant value of $2v_0 = (0.52 \pm 0.03)\mu\text{m}$. This result is very instructive since it implies that the craze thickening at the crack tip does not occur by additional fibrillation of new bulk material and hence it must take place by an enhanced stretching of the already formed fibrils. Together with the results shown in Fig. 5b the magnitude of the strain in the craze can be roughly estimated. The result shows

that between two successive crack jumps the strain on the fibrils at the crack tip increases by the fatigue process from about 130% to about 270% at breakdown. The strain on the fibrils along the craze contour has been analysed in detail after various numbers of loading cycles and it has been found that the strain shows a nearly constant level in that part of the craze which corresponds to the initial craze size just after a crack jump; of course, the strain level increases with loading cycles [14].

The stretching of already formed craze fibrils by more than 100% without any measurable additional fibrillation of bulk material is basically a fatigue process of the craze fibrils. It is absolutely different from the other craze widening process in which additional fibrillation of bulk material occurs. The latter process has been well documented at stationary cracks [15–17] and in real [12] and so-called continuous crack propagation [9] under quasi-static and fatigue loading, respectively. The fatigue process of already formed craze fibrils seems to be the key mechanism causing discontinuous fatigue crack propagation.

With respect to the cracking process between two successive growth bands it has been suggested [3, 18, 19] that cracking occurs by a void coalescence mechanism with the void size distribution reflecting the internal structure of the craze just before crack propagation. In recent SEM investigations, however, using an advanced technique of specimen preparation and thus enabling a higher resolution, it has been found that in PVC the typical structures in the fracture surface consist of different arrangements and differently broken types of craze fibrils [11, 20]. To illustrate this fact a sequence of structures observed on the fracture surface is shown in Fig. 9.

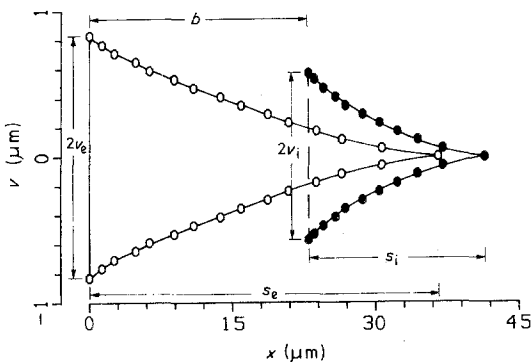


Figure 8 Craze zone at the crack tip under upper load in PVC just before and after crack jump ($\Delta K_{I1} = 0.48 \text{ MN m}^{-3/2}$).

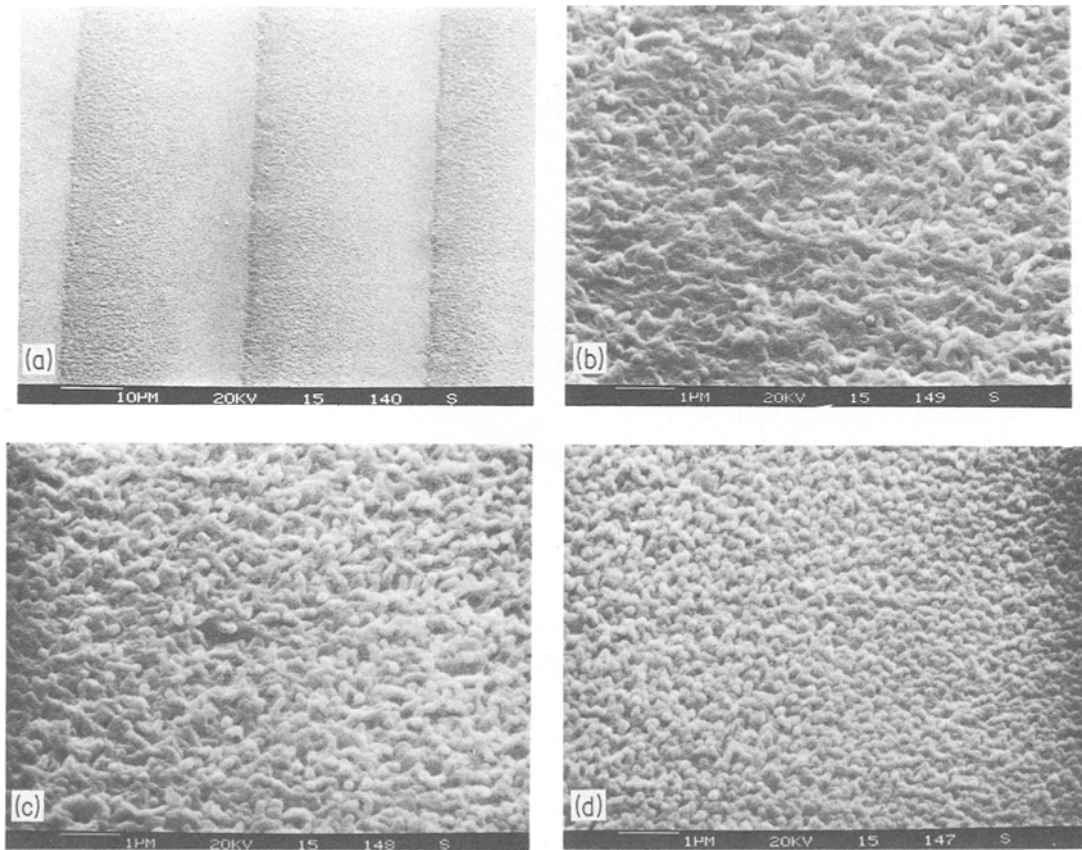


Figure 9 SEM micrographs of discontinuous growth bands in PVC [20] (crack propagation direction from left to right). (a) Overview on several bands; (b) region in front of the middle fatigue line; (c) region in between two fatigue lines; and (d) region ahead of the next fatigue line.

In Fig. 9a an overview is given on several growth bands. The crack propagation direction is normal to the growth bands and in this case from left to right. Details of the central band are given in Figs. 9b to d and they reveal that a band consists of differently broken and deformed craze fibrils. The length of the fibrils becomes shorter going along the band in the crack propagation direction. It has been demonstrated [11] that the arrangement of broken fibrils of different lengths may simulate such structures, which have been formerly interpreted as voids of different size. It can be observed from these photographs and from the published ones [11, 20] that large segments of broken fibrils will form the large holes near to the craze base while the shorter ones will form the small holes near to the craze tip. There are two other observations which may be helpful in this context. First, due to the wedge form of the craze zone a decreasing length of the fibrils is to be

expected along a band; this may be deduced qualitatively from Fig. 8. (However, Fig. 8 cannot be applied strictly since it refers to stretched fibrils whilst in the situation here segments of broken fibrils in the relaxed state are considered.) Secondly, the failure of the fibrils takes place in different geometrical planes; it can be seen from the micrographs that in the region near to the craze base the fibrils fail in an irregular way at one or other side of the interface craze/bulk material giving segments of very different length and, even more important, thus giving additional space between them; in the region near to the craze tip the fibrils fail in the mid-rib giving segments of almost the same length. Thus, the so-called voids in the fracture surface are only different, partly random arrangements of fibrils' segments of various length; they do not reflect the cracking mechanism. Another basic aspect has to be emphasized concerning the relevance of fibrils versus

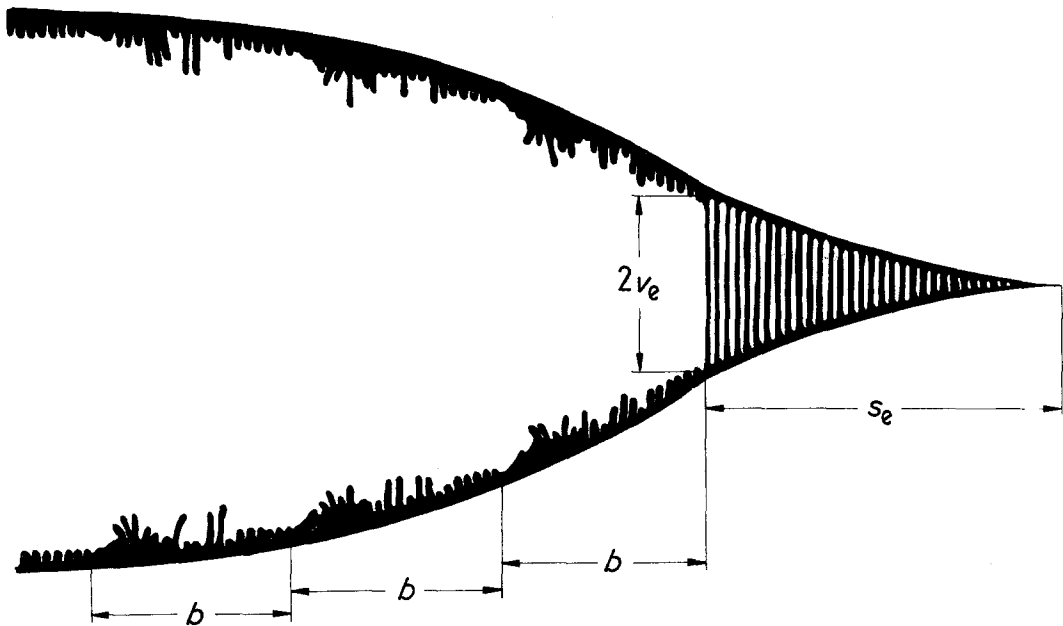


Figure 10 Discontinuous fatigue crack propagation: schematical representation of fibrils stretched in the craze zone and broken in the crack opening.

voids: the craze material is formed by fibrillation of bulk material leading to the still load bearing structure of the crazes.

In front of the fatigue line bundles of highly deformed craze fibrils which are fused together have been observed. From these SEM photographs and the interference optical results the following fracture mechanism in discontinuous FCP has been deduced [11]. At the end of a series of loading cycles, the craze fibrils directly ahead of the crack tip are most deformed and fail by thermal fatigue.

In Fig. 10 the discontinuous fatigue crack propagation is represented schematically showing stretched fibrils in the craze zone and ones broken into different lengths in the crack opening.

3.2.2. Influence of relative stress intensity factor

In the previous section the craze growth behaviour has been investigated mainly between two successive crack jumps and hence under constant ΔK_I . Now the influence of stress intensity on craze dimensions will be determined. This implies that different crazes under different loads have to be considered during discontinuous FCP. Macroscopically the influence of ΔK_I on the discontinuous FCP can be demonstrated by the fact that the number of cycles N between two successive crack jumps decreases strongly with increasing ΔK_I [3,

17]. In Fig. 11 the behaviour of the specific grade of PVC investigated is given. Comparing with other data it has to be taken into account that in PVC the cycle number, N , is strongly dependent on molecular weight [3, 18].

Fig. 12 shows the craze width, $2v$, measured directly at the crack tip as a function of ΔK_I . The maximum craze widths, $2v$, were measured under upper load between successive crack jumps and extrapolated to the situations before ($2v_e$) and after ($2v_i$) a crack jump. $2v_0$ is the craze width under lower load. For all three characteristic craze widths a linear increase with ΔK_I can be seen. This behaviour is quite similar to that found already for continuous crack growth in PMMA (see Fig. 3). However, the slopes in Fig. 12 differ to such a degree, that a quite different straining behaviour of the craze fibrils must be assumed. This is brought out more clearly when the data are expressed in terms of the strain, $\epsilon = (2v - 2v_0) / 2v_0$. Under continuous crack growth in the ΔK_I range investigated, the strain on PMMA craze fibrils grows moderately from about 70 to about 120% with increasing ΔK_I [9]. A completely different situation exists during discontinuous crack growth in PVC, where the strain on the craze fibrils decreases with increasing K_I values. In the situation where the individual fibrils are most severely stretched, just before a crack jump occurs, ϵ

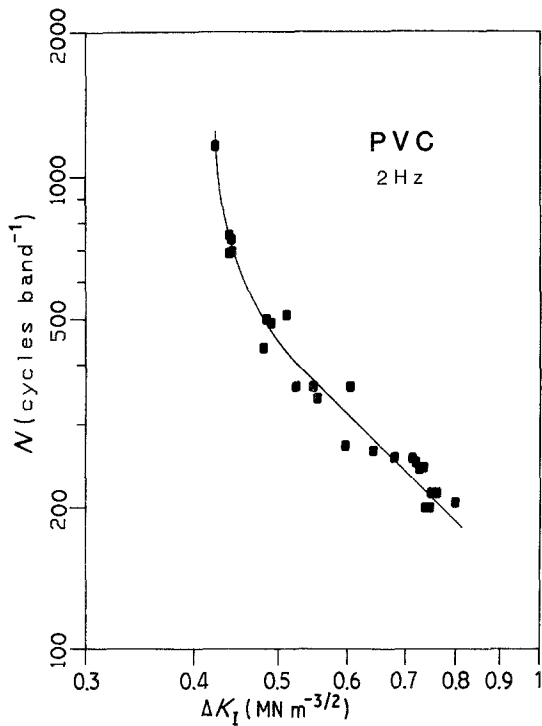


Figure 11 Number N of loading cycles per growth band as a function of ΔK_I .

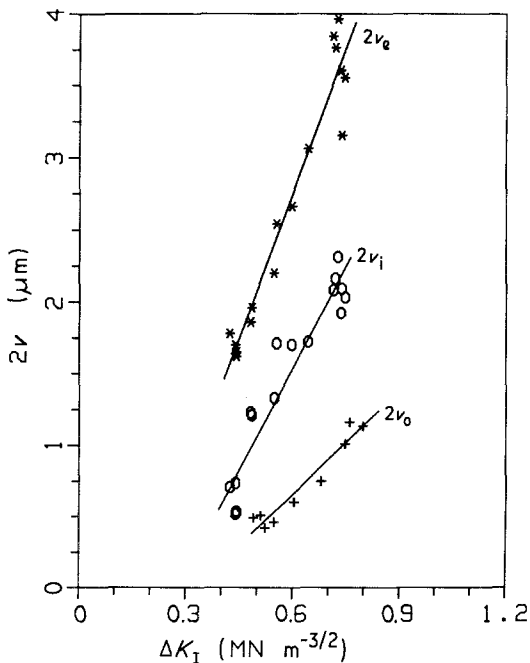


Figure 12 Influence of ΔK_I on craze widths $2v$ at the crack tip in PVC during discontinuous crack growth.

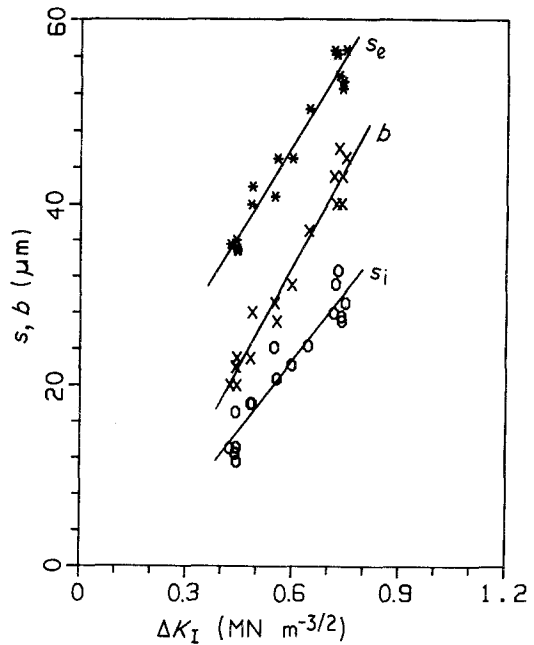


Figure 13 Influence of ΔK_I on craze lengths s and band width b in PVC during discontinuous crack growth.

decreases from about 400% at $\Delta K_I = 0.44 \text{ MN m}^{-3/2}$ to about 250% at $\Delta K_I = 0.76 \text{ MN m}^{-3/2}$. This decrease in strain, ϵ , with increasing ΔK_I may be seen as inherently contradicting the notion that, between two successive crack jumps at constant ΔK_I , the strain on the fibrils increases. The contradiction may be resolved as follows. Just after a crack jump the strain on the already formed fibrils at the crack tip is governed by the fatigue effect, showing an increase in strain with the number N of cycles between two crack jumps. This cycle number, N , decreases with ΔK_I (see Fig. 11) leading to the related decrease of both fibril strain, ϵ , and cycle number, N . An extrapolation of this relationship to just one cycle indicates a strain of about 150%, which corresponds closely to the value determined at continuous crack growth in PMMA under higher ΔK_I levels.

The influence of ΔK_I on craze length, s , in PVC is shown in Fig. 13. Both characteristic craze lengths, s_e just before and s_i just after a crack jump, show a linear increase with ΔK_I , thus leading to a similar result as that observed during continuous fatigue crack growth in PMMA [9]. In Fig. 13 the distances, b , of the crack jumps measured as growth bands on the fracture surface are also given. For a given ΔK_I the sum of band width, b , and initial craze length, s_i , should, in

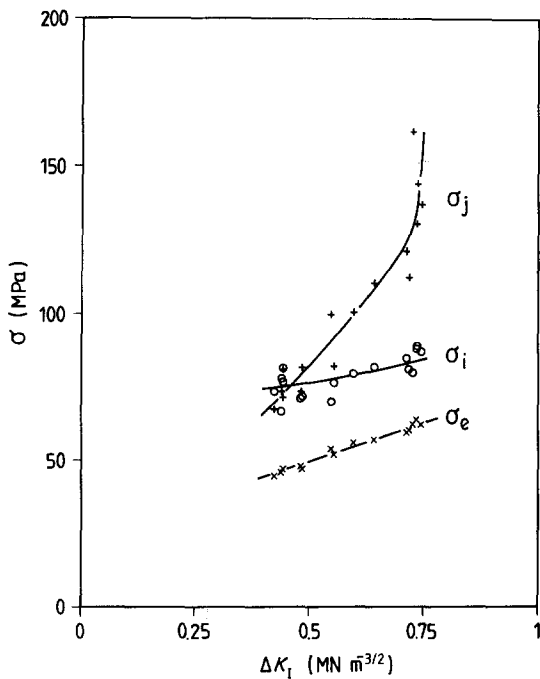


Figure 14 Craze stresses σ referring to different craze length: σ_e to end, σ_i to measured initial, and σ_j to expected initial craze length.

principle, be equal to the craze end length s_e . At low ΔK_I levels this is almost the case. With increasing ΔK_I , however, the sum of b and s_i increasingly exceeds s_e , so that at $\Delta K_I = 0.76 \text{ MN m}^{-3/2}$ the excess amounts to nearly $20 \mu\text{m}$. This effect might be explained as follows. As already noticed in Figs. 5 and 6 an enlargement in craze length occurs at the very moment of the crack jump. The increase in craze length with ΔK_I can be quantitatively explained by application of the Dugdale model. From the Dugdale model it follows that the stress on the craze boundary, and hence on the fibrils, is proportional to ΔK_I and inversely proportional to the square root of craze length. From Fig. 13 it would be expected that the initial craze length, the difference between s_e and b , would be nearly constant. With increasing ΔK_I a constant initial craze length requires that the fibrils would have to bear an increasing stress. The material, therefore, responds by a redistribution of stress which results in an enlarged craze length under lower stress. This can be demonstrated by applying the Dugdale model to the different craze length in calculating the craze stress, σ :

$$\sigma = \left(\frac{\pi}{8} \frac{1}{s} \right)^{1/2} K_I \quad (1)$$

In Fig. 14 the derived craze stresses, σ , as a function of stress intensity factor, K_I , are shown, neglecting the small difference between ΔK_I and K_I . The craze stress, σ_j , refers to that initial craze length as expected theoretically by the difference between the craze length s_e and bandwidth b (compare Fig. 13), while the craze stress, σ_i , refers to the measured initial craze length. It can be seen that the theoretical initial craze stress, σ_i , would increase sharply with ΔK_I . The material, however, reacts by an additional craze growth during the crack jump leading to a lowered almost constant craze stress, σ_i , in the different actual measured initial craze zones. The stress, σ_e , on the end craze zone is still lower by about 20 to 30 MPa than the craze stress, σ_i . It has to be borne in mind that all craze stresses derived above refer to an evaluation by the Dugdale model using a constant stress along the craze contour. For initial craze sizes this modelling by the Dugdale model gives reasonable agreement. There is less agreement when the craze zone approaches its end size. Therefore, a variable stress distribution along the craze seems to give a better fit to these measured craze contours. This "second order correction", however, does not change the principal conclusion of the preceding discussion.

Acknowledgement

The financial support of the Deutsche Forschungsgemeinschaft (DFG) by the program "Physikalische Grundlagen des Fließ- und Deformationsverhaltens von Polymeren" is gratefully acknowledged.

References

1. J. P. ELINCK, J. C. BAUWENS and G. HOMES, *Int. J. Fract. Mech.* 7 (1971) 277.
2. J. A. MANSON and R. W. HERTZBERG, *CRC Crit. Rev. Macromol. Sci.* 1 (1973) 433.
3. R. W. HERTZBERG and J. A. MANSON, "Fatigue of Engineering Plastics" (Academic Press, New York, 1980).
4. *Idem*, *J. Mater. Sci.* 8 (1973) 1554.
5. J. S. HARRIS and I. M. WARD, *J. Mater. Sci.* 8 (1973) 1655.
6. N. J. MILLS and N. WALKER, *Polymer* 17 (1976) 335.
7. R. SCHIRRER, M. G. SCHINKER, L. KÖNCZÖL and W. DÖLL, *Colloid Polym. Sci.* 259 (1981) 812.
8. W. DÖLL, M. G. SCHINKER and L. KÖNCZÖL, "Deformation, Yield and Fracture of Polymers" (Plastics and Rubber Institute, Conference Proceedings, London, 1982) p. 20.1.
9. W. DÖLL, L. KÖNCZÖL and M. G. SCHINKER,

- Polymer* **24** (1983) 1213.
10. G. W. WEIDMANN and W. DÖLL, *Colloid a. Polym. Sci.* **254** (1976) 205.
 11. M. G. SCHINKER, L. KÖNCZÖL and W. DÖLL, *ibid.* **262** (1984) in press.
 12. M. G. SCHINKER and W. DÖLL, "Mechanical Properties at High Rates of Strain" (Institute of Physics, Conference Series No. 47, Bristol, 1979) p. 224.
 13. M. D. SKIBO, R. W. HERTZBERG and J. A. MANSON, *J. Mater. Sci.* **11** (1976) 479.
 14. L. KÖNCZÖL, M. G. SCHINKER and W. DÖLL, Proceedings of 29th International Symposium on Macromolecules, Bucharest, Romania, 1983, Section IV, p. 331.
 15. B. D. LAUTERWASSER and E. J. KRAMER, *Phil. Mag.* **A39** (1979) 469.
 16. N. VERHEULPEN-HEYMANS, *Polymer* **20** (1979) 356.
 17. W. DÖLL, L. KÖNCZÖL and M. G. SCHINKER, *Colloid Polym. Sci.* **259** (1981) 259, 171.
 18. R. W. HERTZBERG, J. A. MANSON and M. D. SKIBO, *Polym. Eng. Sci.* **15** (1975) 252.
 19. C. M. RIMNAC, R. W. HERTZBERG and J. A. MANSON, *J. Mater. Sci. Lett.* **2** (1983) 325.
 20. M. H. SCHINKER, L. KÖNCZÖL and W. DÖLL, *J. Mater. Sci. Lett.* **1** (1982) 475.
 21. M. D. SKIBO, R. W. HERTZBERG, J. A. MANSON and S. L. KIM, *J. Mater. Sci.* **12** (1977) 531.
 22. M. D. SKIBO, J. A. MANSON, R. W. HERTZBERG and E. A. COLLINS, *J. Macromol. Sci. Phys. B* **14** (1977) 525.

*Received 12 August
and accepted 13 September 1983*